

Supplementary Materials. A viscous buoyancy-driven flow modeled by Boundary-Fitted and Immersed-Boundary Methods with the Meso-NH code.

Franck Auguste¹, Géraldine Réa¹, Roberto Paoli^{3,4}, Christine Lac², Valéry Masson², and Daniel Cariolle^{1,2}

¹CECI, CNRS, CERFACS, Toulouse, France

²CNRM, CNRS, Météo-France, Toulouse, France

³University of Illinois at Chicago, Department of Mechanical and Industrial Engineering, Chicago, USA

⁴Argonne National Laboratory, Argonne, USA

Correspondence to: Franck Auguste (franck.auguste@cerfacs.fr)

Abstract.

The *Implementation of an Immersed Boundary Method in the Meso-NH v5.2 model: Applications to an idealized urban-like environment* paper is enriched with a viscous buoyancy-driven flow case (Straka et al., 1993). This additional case presents the comparison of the results obtained by a Boundary-Fitted Method (BFM) and Immersed-Boundary Method (IBM) used in the Meso-NH (MNH) code (Lafore et al., 1998; Lac et al., 2018). This popular case is a thermodynamic one inducing an IB forcing of the energy equation (Eq. 1) presented in the main paper. Note that the comparison of the BFM results with the literature was successfully done in Lunet et al. (2017).

1 Introduction

The thermodynamic case proposed by Straka et al. (1993) is a cold air bubble falling in an idealized atmospheric condition and followed in time by the development of a gravity current above an ideal surface. After recalling the conditions and the hypothesis imposed by the benchmark, the MNH-IBM results are compared to those obtained by MNH-BFM.

This physical case with MNH-BFM was intensively investigated in Lunet et al. (2017) to compare a fifth-order WENO advection scheme to a fourth centered scheme (CEN4), the two showing a good agreement with the literature. In this study, only CEN4 is employed.

The ambient conditions correspond to a neutrally ($\theta = 300K$) stratified dry atmosphere with air initially at rest (see Straka et al, 1993 for details on the reference conditions). Kinematic viscosity is imposed to $\nu_f = 0.1m^2.s^{-1}$. The case satisfies the incompressible or quasi-incompressible hypothesis (low Mach number). The two-dimensional domain is defined by $x \in [0 : 51, 2.10^3]m$ in the horizontal direction and $z \in [0 : 6, 4.10^3]m$ in the vertical direction. The type of lateral boundary conditions is cyclic. Free slip conditions without permeability are applied at the bottom and top surfaces. No relaxation (to avoid reflective waves) is injected in the upper part of the atmosphere. The flow is symmetric with respect to the z axis at $x = 25, 6.10^3m$ (hence

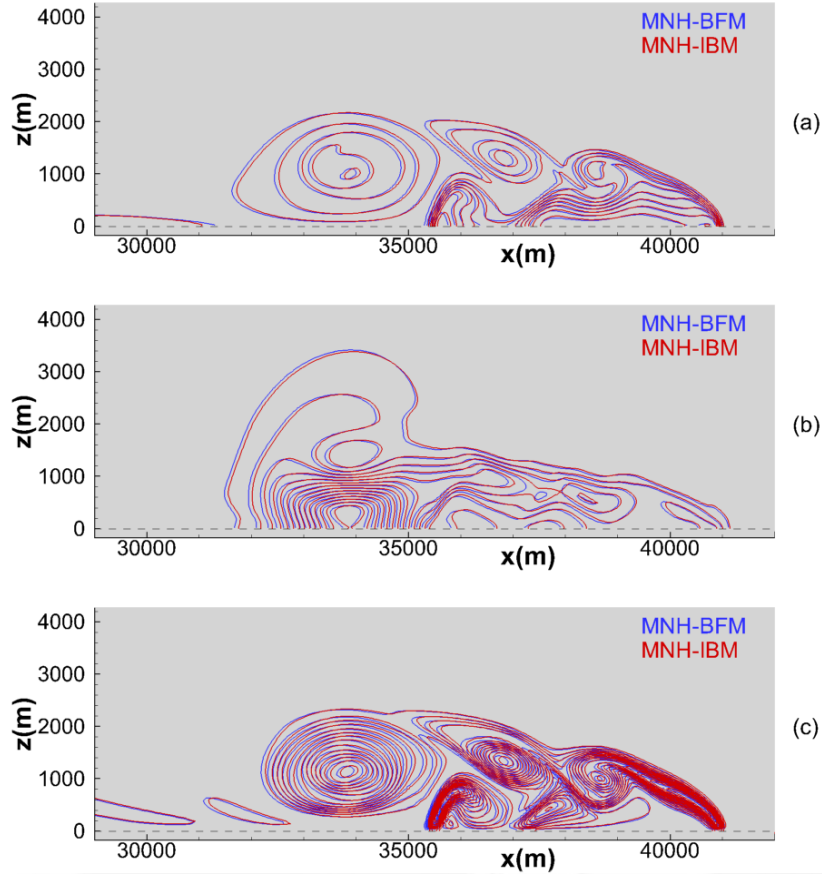


Figure 1. The Straka density current developed at $t = 900\text{s}$: sixteen isocontours of the potential temperature $\theta \in [284 : 299]\text{K}$ (a), the kinetic energy where $e_k \in [0 : 660]\text{ m}^2\text{s}^{-2}$ (b), the enstrophy where $e_s \in [0 : 0.0064]\text{ s}^{-2}$ (c). The blue (resp. red) line corresponds to the MNH-BFM (resp. MNH-IBM) solutions ($\Delta x = 50\text{m}$).

only the results in the region $x > 25,6 \cdot 10^3\text{m}$ are shown). Absolute temperature is initially placed in a region with an elliptic shape and maximum amplitude localized in its center: Location are $(x_c; z_c) = (25, 6; 3) \cdot 10^3\text{ m}$; size is $(x_r; z_r) = (4; 2) \cdot 10^3\text{ m}$; region is $R = \sqrt{\left(\frac{x-x_c}{x_r}\right)^2 + \left(\frac{z-z_c}{z_r}\right)^2}$; amplitude is $\Delta T = -15\cos(\pi R + 1)/2\text{ K}$ if $R < 1$, $\Delta T = 0\text{ K}$ elsewhere.

5 After nine minutes the shear at the front (between the disturbed and undisturbed region) is sufficiently high to initiate a vortex shedding (Kelvin-Helmholtz instability type). After fifteen minutes three vortices are clearly visible. Here we only focus on the flow properties at this particular time. The variables obtained at $t = 900\text{ s}$ are presented in the Table 1.

To obtain a MNH-BFM reference solution a 2048×256 mesh ($\Delta x_{ref} = 25\text{m}$) is built. The time step is fixed to $\Delta t = 0.1\text{s}$: the CFL number respects $\frac{U_{max}\Delta t}{\Delta x} < 0.2$. The results of the MNH-BFM reference solution are in good agreement with those of

Front location	$x_{front} = x - 25600$
Extreme values of the temperature	$\Delta\theta_{min} = \theta_{min} - 300$
Extreme values of the velocity field	$u_{min,max}$ (horizontal direction), $v_{min,max}$ (vertical direction)
Kinetic energy	$e_k = \frac{1}{2} \mathbf{u} ^2$
Enstrophy	$e_s = (\nabla \times \mathbf{u})^2 = \boldsymbol{\omega} ^2$

	$\Delta\theta_{min}$ K	u_{min} $m.s^{-1}$	u_{max} $m.s^{-1}$	v_{min} $m.s^{-1}$	v_{max} $m.s^{-1}$	x_{front} km	$\sum \mathbf{u} ^2$ $m^2.s^{-2}$	$\sum \boldsymbol{\omega} ^2$ $10^{-5}s^{-2}$	ω_{max} $10^{-2}s^{-1}$
$\Delta x = 25m$									
Rosa et al. (2011)	-9.96	-15.29	35.06	-15.94	13.07	15.16			
Straka et al. (1993)	-9.77	-15.19	36.46	-15.95	12.93	15.53	11.18	8.37	
MNH-BFM	-9.66	-15.26	36.14	-15.91	12.93	15.39	10.50	8.15	7.45
$\Delta x = 50m$									
MNH-BFM	-9.66	-15.24	36.11	-15.88	12.89	15.40	10.50	8.09	7.43
MNH-IBM	-9.74	-15.13	36.08	-15.94	13.09	15.41	10.18	7.87	7.41

Table 1. The Straka current: definition of the studied local and integrated variables (top) and comparison (depending on the spatial resolutions) of MNH-IBM, MNH-BFM results and thus of Rosa et al. (2011) and Straka et al. (1993) (bottom).

Straka et al. (1993) and Rosa et al. (2011) using the same spatial resolution regarding the travelled distance by the current, the thermal/kinetic energies and the vorticity production are well-recovered (Table 1).

Using a 1024×128 mesh ($\Delta x_{ref} = 50m$) and $\Delta t = 0.1s$ ($\frac{U_{max}\Delta t}{\Delta x} < 0.1$), the physical problem is simulated with MNH-BFM and MNH-IBM. Note that two additional points are necessary in the vertical direction (below the ground, dashed line in the Figure 1) to compute the ghost points in the IBM version. The convergence in space of the solution is shown Table 1 by the weak differences between MNH-BFM($\Delta x_{ref} = 25m$) and MNH-BFM($\Delta x_{ref} = 50m$). The good agreement BFM/IBM on the density current location and its characteristics at $t = 900s$ is also illustrated in Figure 1 plotting the θ potential temperature (top), the kinetic energy (middle) and the enstrophy (bottom) contours (BFM in blue line; IBM in red line).

Even if the fluid-solid interface is flat in this case, MNH-IBM preserves the change of the potential energy due to the gravitational acceleration in the momentum equation, which reflects the impermeability conditions of the ground due to the Cut-Cell Technique employed in the pressure solver. The slip condition on the tangent velocity and the potential temperature at the ground are also well-insured by the Ghost-Cell Technique.

References

- Lac, C., Chaboureau, J.-P., Masson, V., Pinty, J.-P., Tulet, P., Escobar, J., Leriche, M., and others (2018). Overview of the Meso-NH model version 5.4 and its applications. *Geosci. Model Dev.*, 11, 1929-1969.
- Lafore, J. P., Stein, J., Asencio, N., Bougeault, P., Ducrocq, V., Duron, J., Fisher, C., Hèreil, P., Mascart, P., Masson, V., Pinty, J. P., Redelsperger, J.-L., Richard, E., and Vilà-Gueau de Arellano, J. (1998). The Meso-NH Atmospheric Simulation System. Part I: adiabatic formulation and control simulations. Scientific objectives and experimental design. *Annales Geophysicae*, 16, 90-109.
- 5 Lunet, T., Lac, C., Auguste, F., Visentin, F., Masson, V., and Escobar, J. (2017). Combination of WENO and explicit Runge-Kutta methods for wind transport in Meso-NH model. *Mon. Wea. Rev.*, 145(9), 3817-3838.
- Rosa, B., Kurowski, M., and Ziemiański, M. (2011). Testing the anelastic nonhydrostatic model EULAG as a prospective dynamical core of a numerical weather prediction model Part I: Dry benchmarks. *Acta Geophysica*, 6(59), 1236-1266.
- 10 Straka, JM, Wilhelmson, R. B., Wicker, L. J., Anderson, J. R., and Droegemeier, K. K. (1993). Numerical solutions of a non-linear density current: A benchmark solution and comparisons. *Int. J. for Num. Methods in Fluids*, 17(1), 1-22.